Photophysical Study of New Methanofullerene−TTF Dyads: An Obvious Intramolecular Charge Transfer in the Ground States

Hiroyuki Nishikawa,*,† Shigeru Kojima,† Takeshi Kodama,† Isao Ikemoto,† Shinzo Suzuki,† Koichi Kikuchi,† Mamoru Fujitsuka,‡,§ Hongxia Luo,‡ Yasuyuki Araki,‡ and Osamu Ito*,‡

Department of Chemistry, Graduate School of Science, Tokyo Metropolitan University, Hachioji, Tokyo 192-0397, Japan, and Institute of Multidisciplinary Research for Advanced Materials, Tohoku University, CREST(JST), Katahira, Aoba-ku, Sendai, 980-8577, Japan

Received: October 17, 2003; In Final Form: December 10, 2003

Three isomers of a new C_{60}−TTF dyad—C_{60}−*X*-TTF (*X* = *ortho*, *meta*, and *para*)—have been synthesized by changing the linking positions (*ortho*, *meta*, and *para*) at a phenyl group that is attached to the methano-[60]fullerene. The dyads showed clear intramolecular charge transfer (CT) absorption bands in the steady-state absorption spectra, which was indicative of an intramolecular CT interaction between the C_{60} and TTF moieties in the ground state. The increase in intensity of the CT absorption bands followed the order C_{60}−*ortho*-TTF > C_{60}−*meta*-TTF ≫ C_{60}−*para*-TTF, which can be reasonably explained by the optimized molecular structures that are calculated at the ab initio level. Extreme quenching of the fluorescence intensity from the locally excited C_{60} moiety was observed to follow the aforementioned order, which suggests that very fast excited singlet-state dynamics are dependent on the isomers. The quenching of the absorption intensities of the triplet state of the C_{60} moiety detected in the nanosecond region was also observed to follow the same order, which suggests that competitive paths that are more efficient than intersystem crossing are present. From subpicosecond transient absorption measurements, very short-lived transient absorption bands attributed to the overlap of S_1−S_n with the excited CT state that has strong CT character were obtained for C_{60}−*ortho*-TTF (and C_{60}−*meta*-TTF); appreciable charge-separated (CS) species were generated for C_{60}−*para*-TTF. The lifetimes of the CT and CS states increased in the order of C_{60}−*ortho*-TTF < C_{60}−*meta*-TTF < C_{60}−*para*-TTF. Overall, it was revealed that the ground and excited states are controlled by the difference in proximity between the C_{60} and TTF moieties, depending on the linking positions.

1. Introduction

Chemically functionalized fullerenes are considered to be promising materials in various research fields, and considerable research has been conducted on the chemistry of fullerenes.[1,2] Recently, donor−acceptor dyad systems that are based on C_{60} as an acceptor unit have attracted appreciable attention, from the viewpoint of potential applications in molecular electroactive devices and as model compounds for artificial photosynthesis.[2−7] The C_{60} moiety in such dyad systems retains most of the known important redox properties, as well as photophysical properties; the low reorganization energy of C_{60} affords various unique photoinduced phenomena, such as fast charge separation (CS) and slow charge recombination (CR) in C_{60}-based systems.[5−7] In fact, several donor-linked C_{60} derivatives fabricated on electrodes displayed photovoltaic property,[8] and some of them were used in self-assembled monolayers to realize high solar energy conversion efficiency.[9]

Generally, efficient photoinduced CS and the following long-lived CS state are required by the component molecules of photoactive devices. Among the donor components of C_{60} dyad systems, tetrathiafulvalene (TTF) derivatives are regarded as valuable molecules, because C_{60}−TTF dyads are considered to have a stable CS state, because of the redox property of the TTF core as a Weitz-type donor,[10] which consists of a multistage redox system and gains aromaticity upon oxidation.[7b] In regard to the development of photoelectric devices, intermolecular migration of charge carriers is also an important factor for photocurrent generation. In this context, TTF derivatives are as prominent as C_{60}, because they are significant donor molecules for producing the highly electrically conductive materials with a variety of interesting electronic ground states, such as superconductivity.[11] The synthesis of several C_{60} dyads linked with TTF has been reported, and, for some, the precise photophysical properties also have been reported.[12−31] C_{60}−TTF dyads with relatively long-lived CS states have been successfully prepared. In particular, the lifetimes of C_{60} dyads linked with π-extended TTF (C_{60}−exTTF) are several hundred nanoseconds,[13,23] and recently, a donor−acceptor system that incorporates fluorofullerene and extended TTF is reported to have a long-lived CS state with a lifetime of hundreds of nanoseconds also.[32] Furthermore, the C_{60}−exTTF triad is reported to exhibit an unusually long lifetime—111 μs—that results from a stepwise mechanism in the CR process.[33] However, relatively weak or no charge transfer (CT) interaction between the C_{60} and TTF moieties in the ground state has been reported for the C_{60}−TTF dyads examined so far, although they exhibited intramolecular CT upon photo irradiation, namely, in the excited state.

* Authors to whom correspondence should be addressed. E-mails: hiron@comp.metro-u.ac.jp, ito@tagen.tohoku.ac.jp.
† Tokyo Metropolitan University.
‡ Tohoku University.
§ Present address: The Institute of Scientific and Industrial Research, Osaka University, Ibaraki, Osaka 567-0047, Japan.

10.1021/jp037145n CCC: $27.50
Published on Web 02/21/2004

CHART 1: Molecular Structures of C_{60}−*X*-TTF (*X* = *ortho, meta,* and *para*), C_{60}-Reference, and TTF-Reference

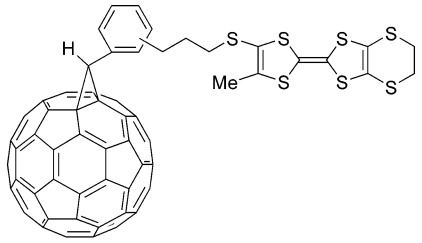

C_{60}-*X*-TTF (*X* = *ortho, meta,* and *para*)

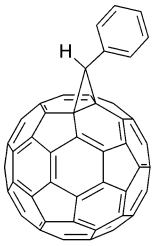

C_{60}-reference

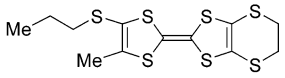

TTF-reference

In this paper, we report the synthesis and the electrochemical and photophysical properties of new C_{60}−TTF dyads, C_{60}−*X*-TTF (*X* = *ortho*, *meta*, and *para*), which show clear intramolecular CT interaction in the ground state, unlike hitherto known C_{60}−TTF dyads. The TTF moiety was linked via a propyl chain to three different positions (*ortho*, *meta*, and *para*) on a phenyl group that was attached to methanofullerene (Chart 1). For C_{60}−*X*-TTF (*X* = *ortho* and *meta*), intramolecular CT absorption bands were clearly observed in the steady-state absorption spectra, and the intensities of the bands increased drastically in the order of C_{60}−*ortho*-TTF > C_{60}−*meta*-TTF ≫ C_{60}−*para*-TTF, which is attributable to the relative distance between the C_{60} and TTF moieties. Ab initio calculations gave the geometrical features of the three isomers, which could reasonably explain the results of the steady-state absorption spectra. To obtain further insight into the dynamic processes in excited states that involve excited CT and CS states of C_{60}−*X*-TTF, time-resolved photolysis spectroscopies were performed in the nanosecond and subpicosecond regions.

2. Results and Discussion

2.1. Synthesis. Synthesis of the three structural isomers, C_{60}−*X*-TTF (*X* = *ortho*, *meta*, and *para*), was performed via the cycloaddition of diazo compounds to C_{60}, as shown in Scheme 1.[34] The cyanoethyl-protected tetrathiafulvalene (**1**)[35] was converted to acetals (**3a**−**c**) by deprotection with 2 equiv of sodium methoxide in methanol, followed by treatment with the respective iodide (**2a**−**c**).[36] Deprotection of the dioxane group in the acetals (**3a**−**c**) with *p*-toluenesulfonic acid afforded the corresponding aldehydes (**4a**−**c**), which were converted to *p*-tosylhydrazones (**5a**−**c**). Diazo compounds (**6a**-**c**) that were required for cycloaddition to C_{60} were generated in situ from **5a**−**c** by treatment with sodium methoxide and readily reacted with C_{60} in refluxing toluene to give C_{60}−*X*-TTF dyads. Dyads were purified by column chromatography (silica gel, carbon disulfide), and subsequent high-performance liquid chromatography (HPLC) using a Buckyprep column and toluene as an eluent to separate them completely from unreacted C_{60}.

According to the position of methano-bridging, there are three isomers for methanofullerenes: two kinetically controlled [5,6]-open isomers and a thermodynamically stable [6,6]-closed isomer, which are distinguishable using the ^{1}H NMR signal of the methine proton.[37] The prepared dyads (C_{60}−*X*-TTF) exhibited a singlet ^{1}H NMR signal of methine resonance at ∼4.0 ppm, which suggests that the dyads have the [6,6]-junction structure. Thermodynamically favored [6,6] isomers reportedly were directly obtained from diazo precursors under refluxing conditions in toluene.[13a]

2.2. Electrochemical Properties. Electrochemical properties of C_{60}−*X*-TTF (*X* = *ortho*, *meta*, and *para*) were investigated by cyclic voltammetry in benzonitrile at 25 °C. The cyclic voltammogram of C_{60}−*ortho*-TTF, as a representative example, is shown in Figure 1, and the redox potentials for all isomers

SCHEME 1: Synthesis of C_{60}−*X*-TTF (*X* = *ortho, meta,* and *para*)

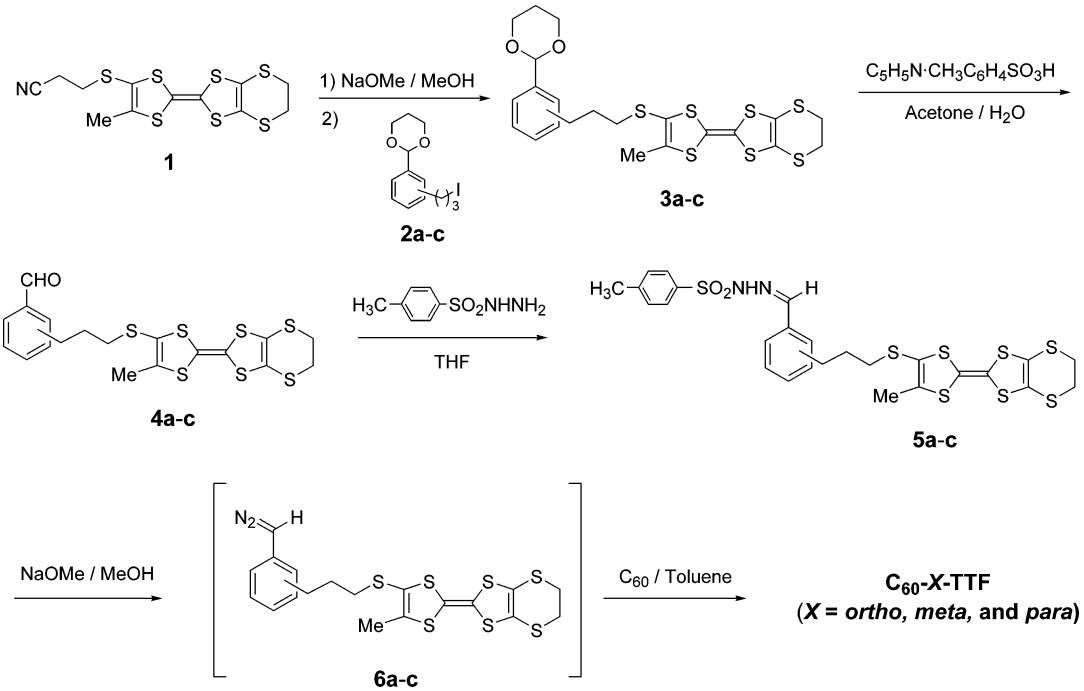

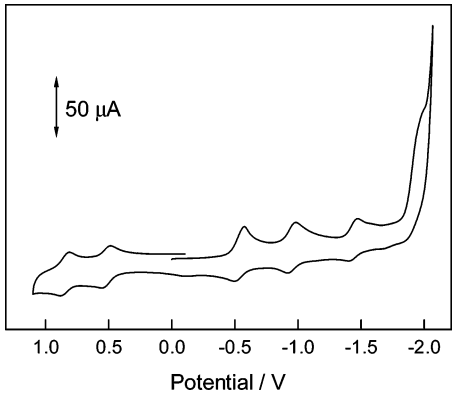

Figure 1. Cyclic voltammogram of C_{60}−*ortho*-TTF in benzonitrile containing 0.1 M *n*-Bu_4NClO_4 (V vs SCE). Scan rate was 50 mV/s.

TABLE 1: Redox Potentials of C_{60}−*X*-TTF (*X* = *ortho*, *meta*, and *para*), TTF-Reference, C_{60}-Reference, and C_{60}[a]

compound	E_1^{ox}	E_2^{ox}	E_1^{red}	E_2^{red}	E_3^{red}	E_4^{red}
C_{60}−*ortho*-TTF	0.52	0.84	−0.54	−0.95	−1.44	−2.00[b]
C_{60}−*meta*-TTF	0.49	0.81	−0.55	−0.95	−1.47	−2.01[b]
C_{60}−*para*-TTF	0.48	0.80	−0.52	−0.95	−1.46	−2.00[b]
TTF-reference	0.45	0.83				
C_{60}-reference			−0.52	−0.95	−1.43	−2.03[b]
C_{60}			−0.49	−0.92	−1.39	−1.89

[a] Given in volts versus a saturated calomel electrode (SCE); 0.1 M *n*-Bu_4NClO_4 in benzonitrile; platinum electrode. [b] Irreversible step.

are summarized in Table 1, together with those of the TTF-reference sample, the C_{60}-reference sample, and C_{60}, for comparison. All the dyads exhibited three pairs of reversible redox waves and one irreversible wave on the reduction side, and two pairs of reversible waves on the oxidation side. The reduction steps correspond to the reduction of the C_{60} moiety, whereas the oxidation steps correspond to the TTF unit, which is in good agreement with the molecular orbital calculation (vide infra); namely, the highest occupied molecular orbital (HOMO) is localized on the TTF moiety and the lowest unoccupied molecular orbital (LUMO) spreads on the C_{60} core. The first reduction potentials for C_{60}−*X*-TTF (*X* = *ortho* and *meta*) are slightly more negative than those of C_{60}-reference and C_{60}−*para*-TTF. Such negative shifts of the E_1^{red} indicates the decrease of electron accepting ability, which may be rationalized by the partial CT from the TTF to the C_{60} moieties.

Compared with the oxidation potentials of TTF-reference, the first oxidation potentials (E_1^{ox}) of C_{60}−*X*-TTF substantially shift to more-positive values and the degree of shift follows the order C_{60}−*ortho*-TTF > C_{60}−*meta*-TTF > C_{60}−*para*-TTF. The positive shifts of the E_1^{ox} obtained for C_{60}−*X*-TTF dyads, in comparison to TTF-reference indicate the decrease of electron donating ability, which may also be rationalized by the partial CT from the TTF to the C_{60} moieties.

2.3. Steady-State Absorption Measurements. Absorption spectra of C_{60}−*ortho*-TTF, C_{60}-reference, and TTF-reference in benzonitrile are shown in Figure 2a. In addition to the local excitation of the TTF moiety at 460 nm and the C_{60} moiety at 550 and 600 nm, a new broad absorption band that corresponds to CT interaction appeared in the region of 700−900 nm, with a clear peak at 750 nm, which suggests that a substantial intramolecular interaction between the C_{60} and TTF moieties exists in the ground state. The absorption coefficient of this CT band is independent of the concentration in the range of 0.02−2.0 mM; therefore, the CT interaction can be assigned to an intrinsic intramolecular one. As shown in Figure 2b, C_{60}−*meta*-TTF and C_{60}−*para*-TTF showed a similar CT band in the

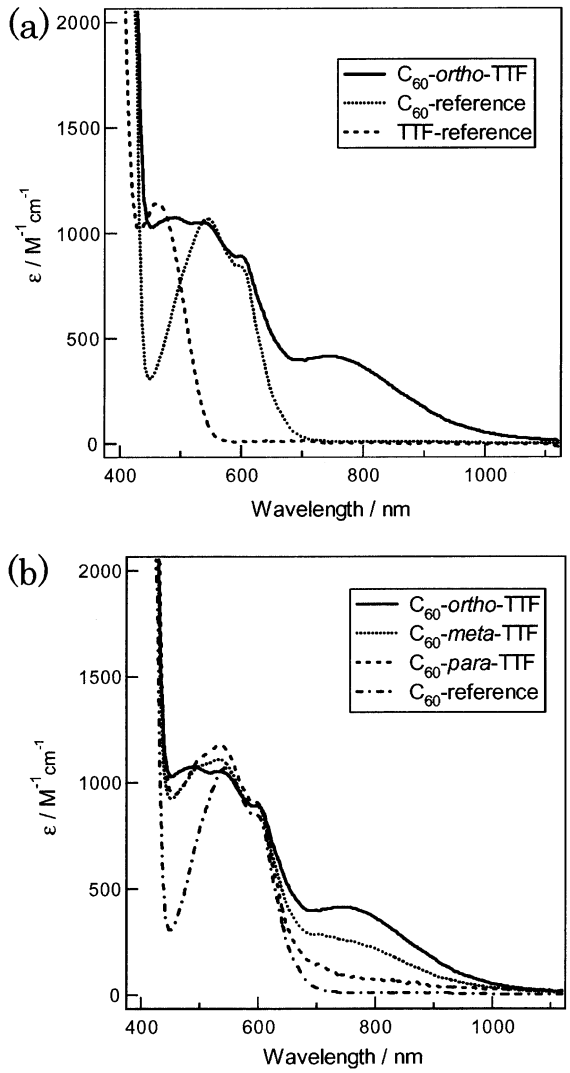

Figure 2. (a) Absorption spectra of C_{60}−*ortho*-TTF, C_{60}-reference, and TTF-reference in benzonitrile (0.2 mM). (b) Absorption spectra of C_{60}−*ortho*-TTF (0.2 mM), C_{60}−*meta*-TTF (0.1 mM), C_{60}−*para*-TTF (0.1 mM), and C_{60}-reference (0.1 mM) in benzonitrile.

700−900 nm region; however, the absorption band of C_{60}−*para*-TTF was a considerably weak shoulder, unlike the cases of the *ortho* and *meta* derivatives. The intensity of the CT absorption bands followed the order C_{60}−*ortho*-TTF > C_{60}−*meta*-TTF ≫ C_{60}−*para*-TTF, which is probably the order of proximity between the C_{60} and TTF moieties. Note that C_{60}−*ortho*-TTF and C_{60}−*meta*-TTF showed clear CT absorption bands in the ground states, in contrast to the C_{60}−TTF dyads reported previously, in which a rather small enhancement of absorption in the CT band region[17,20b,29] or no CT absorption[12−14,18a,23−27] was observed.

In the present laser photolysis studies, as described later, 532- and 388-nm laser lights were used as the excitation source. With the laser excitation at 532 nm, the C_{60} moiety was predominantly (ca. 80%) excited. On the other hand, the 388-nm laser light excited both the C_{60} entity and the TTF moiety. After the laser light irradiation at 532 nm, the absorption spectrum was practically unchanged, which suggests the photostability of C_{60}−*X*-TTF.

2.4. Steady-State Fluorescence Spectra. Figure 3 displays the fluorescence spectra of C_{60}−*X*-TTF (*X* = *ortho*, *meta*, and *para*) and C_{60}-reference observed by excitation at 520 nm in toluene. The C_{60}-reference and C_{60}−*X*-TTF (*X* = *ortho*, *meta*,

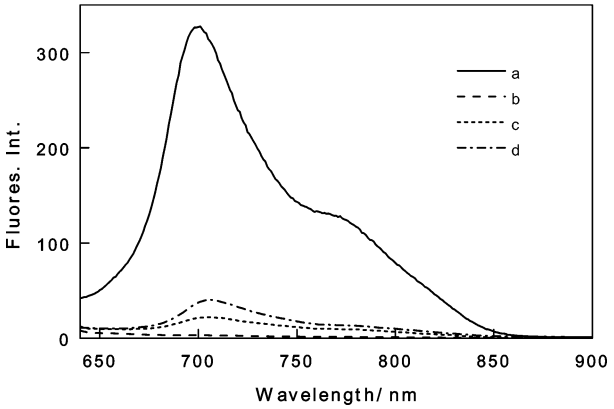

Figure 3. Steady-state fluorescence of (a) C_{60}-reference (0.1 mM), (b) C_{60}−*ortho*-TTF (0.1 mM), (c) C_{60}−*meta*-TTF (0.1 mM), and (d) C_{60}−*para*-TTF (0.1 mM) in toluene. $\lambda_{ex} = 520$ nm.

TABLE 2: Wavelength at Peak Maximum of Charge-Transfer Absorption Band (λ_{CT}), Energy Level of Excited Charge-Transfer States (E_{CT*}), Fluorescence Peak (λ_{FL}), Fluorescence Quantum Yield (Φ_{FL}), and Free-Energy Change for Charge Separation ($-\Delta G_{CS}$) of C_{60}−*X*-TTF (*X* = *ortho*, *meta*, and *para*) and C_{60}-Reference

			fluorescence		
solvent	λ_{CT} (nm)	E_{CT*}[a] (eV)	λ_{FL} (nm)	Φ_{FL}	$-\Delta G_{CS}$[b] (eV)
C_{60}-Reference					
toluene			700	7.00×10^{-4}	
benzonitrile			700[c]	6.00×10^{-4}[c]	
C_{60}−*ortho*-TTF					
toluene	770	1.61	706[e]	0.02×10^{-4}[e]	0.35
benzonitrile	750	1.65	707[c,e]	0.03×10^{-4}[c,e]	0.85
C_{60}−*meta*-TTF					
toluene	750	1.65	706	0.11×10^{-4}	0.33
benzonitrile	740	1.68	707[c]	0.11×10^{-4}[c]	0.85
C_{60}−*para*-TTF					
toluene	[d]	[d]	706	0.21×10^{-4}	0.20
benzonitrile	[d]	[d]	707	0.13×10^{-4}	0.83

[a] $E_{CT*} = 1240/\lambda_{CT}$. [b] $-\Delta G_{CS} = \Delta E_{0-0} - (-\Delta G_{CR})$, where $-\Delta G_{CR} = E_{ox} - E_{red} + \Delta G_S$ ($\Delta G_S = e^2/(4\pi\epsilon_0)\{[1/(2R^+) + 1/(2R^-) - 1/R_{cc}](1/\epsilon_s) - [1/(2R^+) + 1/(2R^-)](1/\epsilon_r)\}$) and ΔE_{0-0} is the energy of the 0−0 transition of C_{60}; E_{ox} and E_{red} are the first oxidation potential of the donor (TTF-reference) and the first reduction potential of the acceptor (C_{60}-reference) in benzonitrile, respectively (R^+ and R^- are radii of the ion radicals of TTF (4.7 Å) and C_{60} (5.6 Å),[40] respectively; R_{cc} is the center-to-center distance between the two moieties; and ϵ_s and ϵ_r are static dielectric constants of solvent used for photophysical studies and the redox measurements). [c] In tetrahydrofuran (THF), because unidentified fluorescence appeared in benzonitrile when the sensitivity of the fluorescence spectrometer was increased. [d] Almost flat. [e] Very weak fluorescence peak.

and *para*) showed fluorescence peaks at ∼700 and 770 nm (shoulder), which are typical peaks for monoadduct derivatives of C_{60}, suggesting that the emissions result from the singlet excited state of the C_{60} moiety ($^1C_{60}^*$−*X*-TTF). Compared with the fluorescence of C_{60}-reference, considerable quenching of the fluorescence intensity of the C_{60} moiety was observed for C_{60}−*X*-TTF, and the fluorescence intensities followed the order C_{60}−*ortho*-TTF ≪ C_{60}−*meta*-TTF < C_{60}−*para*-TTF. The quantum yields (Φ_{FL}), calculated on the basis of the reported value,[14a,38] are summarized in Table 2. This order is exactly the opposite of that for the absorption intensity of the CT band. Thus, we tentatively consider that isomer dependence of the quenching of fluorescence intensity results from the intramolecular CT interaction between the TTF moiety and the photoexcited C_{60} moiety. Namely, the intramolecular CT

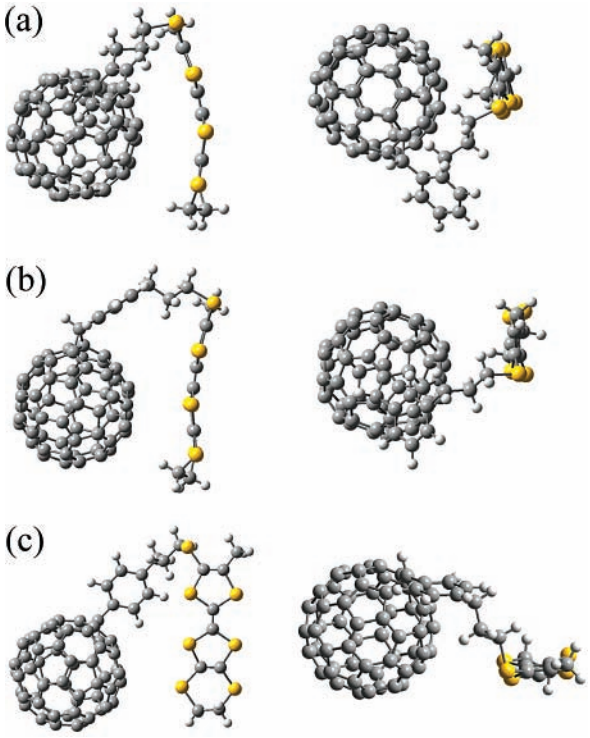

Figure 4. Ab initio HF/3-21G calculated geometric structures of (a) C_{60}−*ortho*-TTF, (b) C_{60}−*meta*-TTF, and (c) C_{60}−*para*-TTF.

interaction of C_{60}−*X*-TTF in the ground state leads to the nonfluorescent excited state of C_{60}−*X*-TTF, probably because of the high degree of CT character in the excited state, even in a nonpolar solvent. Notably, extra new fluorescence was not observed in the wavelength region of >850 nm, which suggests the absence of exciplex fluorescence.[39] It was very difficult to evaluate the fluorescence lifetimes of C_{60}−*X*-TTF, because of very weak fluorescence; the fluorescence lifetimes probably are <10 ps, which was the limit of our instrument. Similar results were obtained in polar solvents.

2.5. Optimized Structures and Molecular Orbital Calculations. To obtain geometrical insight, especially the proximity between the C_{60} and TTF moieties, molecular orbital calculations were performed at the Hartree−Fock theory with a 3-21G basis set using the Gaussian-98 program[41] for C_{60}−*X*-TTF (*X* = *ortho*, *meta*, and *para*). The optimized molecular structures are shown in Figure 4. In the optimized structure of C_{60}−*ortho*-TTF, the center-to-center distance between the TTF and C_{60} entities (R_{cc}, from the center of the central double bond of TTF to the center of the C_{60} spheroid) is estimated to be 9.46 Å. On the other hand, the edge-to-edge distance (R_{ee}, from the center of the central double bond of TTF to the closest C atom on the C_{60} sphere) is estimated to be 3.8 Å. The TTF moiety of C_{60}−*ortho*-TTF slightly bends to fit the round-shaped C_{60} moiety, whereas such a curving of the TTF moiety is not observed for C_{60}−*meta*-TTF and C_{60}−*para*-TTF. The concave structure of the TTF molecule was reported in the crystal of $(BEDT-TTF)_2C_{60}$, in which CT occurs from BEDT−TTF to C_{60}.[42] The relatively short distance between the C_{60} and TTF moieties and the concave molecular structure of the TTF moiety indicate that appreciable electronic interaction exists in the ground state of C_{60}−*ortho*-TTF. For C_{60}−*meta*-TTF, $R_{ee} = 4.3$ Å and $R_{cc} = 9.88$ Å; these distances are slightly longer than those of C_{60}−*ortho*-TTF, but the molecular plane of the TTF moiety faces the C_{60} sphere. Consequently, the π-orbital of TTF (HOMO, vide infra) can interact with the π^*-orbital of C_{60} (LUMO, vide infra).

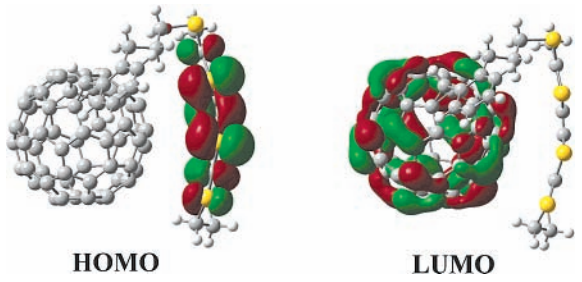

Figure 5. HOMO and LUMO, calculated at the HF/3-21G level of C_{60}−*ortho*-TTF.

Furthermore, the flexibility of the alkyl chain allows C_{60}−*ortho*-TTF and C_{60}−*meta*-TTF to take such orientations with the relatively close distances between the C_{60} and TTF entities, causing intramolecular CT interaction. On the other hand, the R_{ee} and R_{cc} distances of C_{60}−*para*-TTF are much longer (R_{ee} = 6.9 Å, R_{cc} = 12.5 Å), compared with those of C_{60}−*ortho*-TTF and C_{60}−*meta*-TTF. In addition, the TTF plane lies in the upright position against the C_{60} sphere. As a result, the π-orbital of TTF is orthogonal to p-orbitals of C atoms that are situated on the near side of the C_{60} sphere to the TTF moiety. However, it is noted that the shortest distance from the S atom of TTF on the C_{60} side to the nearest C atom on the C_{60} spheroid is 4.2 Å, which suggests a weak interaction with the π^*-orbital of C_{60} through the n-orbital on the S atom in the TTF moiety. The geometrical features in C_{60}−*X*-TTF are completely consistent with the results of the steady-state absorption and steady-state fluorescence measurements; viz., the intensity of CT absorption bands was on the order of C_{60}−*ortho*-TTF > C_{60}−*meta*-TTF ≫ C_{60}−*para*-TTF, along with the strength of CT interaction in the ground state. On the other hand, the fluorescence intensity followed the order C_{60}−*ortho*-TTF < C_{60}−*meta*-TTF ≪ C_{60}−*para*-TTF, which suggests the same order of the CT interaction in the excited state as that in the ground state.

The HOMO and LUMO of C_{60}−*ortho*-TTF are shown in Figure 5. Similar to the C_{60}−TTF dyads reported previously,[12b,13b,22b,29] the HOMO is located on the TTF plane, whereas the LUMO is located on the C_{60} framework. Unfortunately, the contribution of CT characters to the HOMO and LUMO is not determined in the MO calculations at the Hartree−Fock level with the 3-21G basis set.

2.6. Nanosecond Transient Absorption Measurements. Transient absorption spectra of C_{60}−*X*-TTF (*X* = *ortho*, *meta*, and *para*) and C_{60}-reference in the nanosecond region were measured by nanosecond laser photolysis, using 532-nm laser irradiation in benzonitrile (Figure 6). The C_{60}-reference exhibited an absorption peak at 720 nm and a shoulder peak at 820 nm, which are characteristic of the triplet state of the C_{60} moiety.[43] From the time profile in a deaerated solution (shown in the inset of Figure 6), the lifetime of the triplet state of C_{60}-reference, ^{3}(C_{60}-reference)*, was evaluated to be 5.3 μs, which is shorter than the lifetimes for other C_{60} derivatives.[43] The quantum yield (Φ_T) of the triplet state was calculated to be 0.35, from the initial absorbance at 720 nm, using the assumption that the molar extinction coefficient is 12 000 cm^{-1} M^{-1} at 720 nm.[44]

For C_{60}−*X*-TTF (*X* = *ortho*, *meta*, and *para*) in benzonitrile, although transient absorption bands are quite similar to the triplet state of C_{60}-reference, which is indicative of the formation of the triplet state of the C_{60} moiety, $^3C_{60}{}^*$−*X*-TTF, the absorption intensities of the C_{60}−*X*-TTF were quite weak, especially for C_{60}−*ortho*-TTF, in comparison with the initial intensity at 720 nm in the spectra of the C_{60}-reference. Consequently, the Φ_T values estimated from the initial intensities at 720 nm were

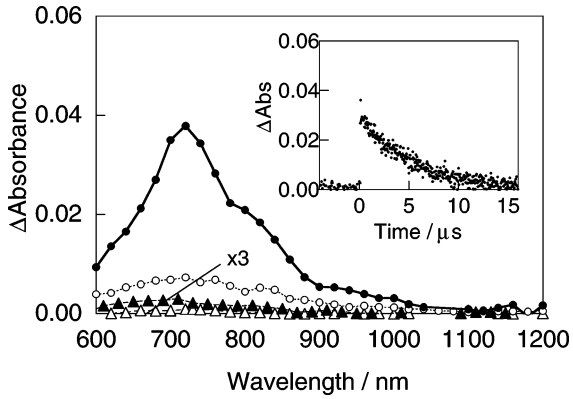

Figure 6. Nanosecond transient absorption spectra of C_{60}-reference in benzonitrile after pulse irradiation using 532-nm light: (●) C_{60}-reference, (○) C_{60}−*para*-TTF, (▲) C_{60}−*meta*-TTF, and (Δ) C_{60}−*ortho*-TTF. Inset shows a time profile at 720 nm of C_{60}-reference.

TABLE 3: Quantum Yield (Φ_T) and Lifetime (τ_T) for $^3C_{60}{}^*$ from the Nanosecond Transient Absorption Band at 720 nm and Fast Decay Rate Constant (k_{decay}) and Lifetime (τ_{decay}) of the Transient Band at 980 nm in Subpicosecond Transient Absorption Measurements of C_{60}−*X*-TTF (*X* = *ortho*, *meta*, and *para*) and C_{60}-Reference

solvent	Φ_T	τ_T (μs)	k_{decay} (s^{-1})	τ_{decay} (ps)
		C_{60}-Reference		
toluene	0.40	17.9		
benzonitrile	0.35	5.3		
		C_{60}−*ortho*-TTF		
toluene	<0.001		1.3×10^{11}	8
benzonitrile	0.003	3.7	3.0×10^{11}	3
		C_{60}−*meta*-TTF		
toluene	0.004	2.6	1.0×10^{11}	10
benzonitrile	0.009	1.8	1.0×10^{11}	10
		C_{60}−*para*-TTF		
toluene	0.070	1.0	8.2×10^{10}	12
benzonitrile	0.068	3.8	8.5×10^{10}	12

extremely low: 0.003, 0.009, and 0.068 for the *ortho*, *meta*, and *para* derivatives, respectively. The time profile gave the lifetime of the triplet states in the *ortho*, *meta*, and *para* derivatives to be 3.7, 1.8, and 3.8 μs, respectively, which are almost the same as that of the triplet state of C_{60}-reference. In nonpolar toluene, transient spectra similar to those in benzonitrile were observed. The Φ_T values and the lifetimes of $^3C_{60}{}^*$−*X*-TTF are summarized in Table 3, together with those in benzonitrile.

The appearance of the triplet state of C_{60}-reference indicates that the triplet state is formed by an intersystem crossing (ISC) process from the singlet excited state of the C_{60} moiety, whose lifetime is ca. 1.2 ns.[43] The low Φ_T values of $^3C_{60}{}^*$−*ortho*-TTF indicate that there is a competitive path with the ISC, such as formation of the excited CT state [($C_{60}{}^{\delta-}$−*ortho*-$TTF^{\delta+}$)*] from $^1C_{60}{}^*$−*ortho*-TTF. For C_{60}−*meta*-TTF, it is reasonable to consider that $^3C_{60}{}^*$−*meta*-TTF should also be formed from $^1C_{60}{}^*$−*meta*-TTF, which may also be competitive with the path to ($C_{60}{}^{\delta-}$−*meta*-$TTF^{\delta+}$)*. The appearance of $^3C_{60}{}^*$−*para*-TTF may be attributed to the ISC process from $^1C_{60}{}^*$−*para*-TTF, which may be competitive with the charge-separation (CS) process, generating $C_{60}{}^{\bullet-}$−*para*-$TTF^{\bullet+}$, because of the weaker CT interaction of C_{60}−*para*-TTF in the ground state, compared with C_{60}−*ortho*-TTF and C_{60}−*meta*-TTF.

The lifetimes of $^3C_{60}{}^*$−*X*-TTF were slightly shorter than that of ^{3}(C_{60}-reference)*, which was also characteristic of C_{60}−*X*-TTF; in $^3C_{60}{}^*$−*X*-TTF, there may be appreciable interaction between the $^3C_{60}{}^*$ moiety with the TTF moiety in close position.

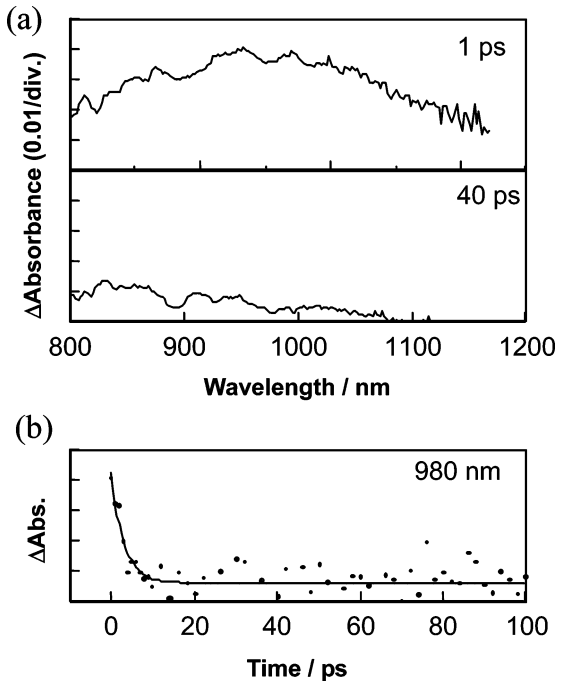

Figure 7. (a) Subpicosecond transient absorption spectra of C_{60}−*ortho*-TTF in benzonitrile after 150-fs pulse irradiation with 388-nm laser light. (b) Time profile at 980 nm.

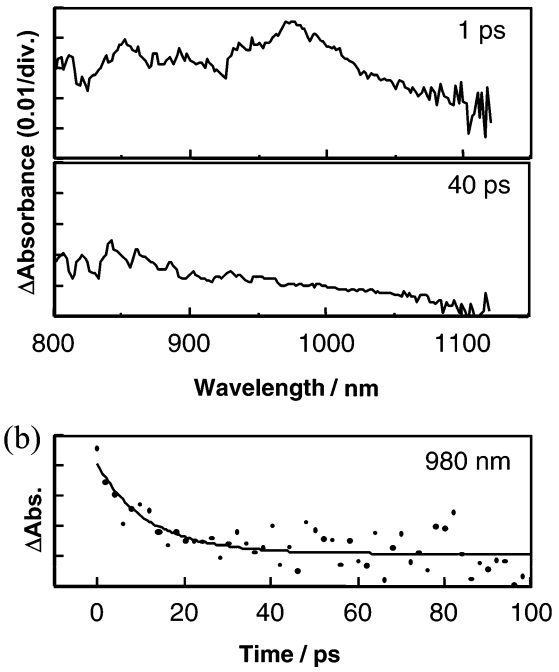

Figure 8. (a) Subpicosecond transient absorption spectra of C_{60}−*para*-TTF in benzonitrile after 150-fs pulse irradiation with 388-nm laser light. (b) Time profile at 980 nm.

2.7. Subpicosecond Transient Absorption Measurements. To probe the dynamic processes in the excited states, a laser photolysis study that used the 150-fs laser pulse was conducted for C_{60}−*X*-TTF (*X* = *ortho*, *meta*, and *para*). Figure 7a shows the subpicosecond transient absorption spectra of C_{60}−*ortho*-TTF in benzonitrile obtained by 388-nm laser light irradiation. In the transient spectrum at 1 ps after the 150-fs laser pulse, a broad absorption band appeared in the region of 800−1200 nm. At 40 ps, almost the broad absorption disappeared, leaving weak absorption bands. The time profile of broad absorption band at 980 nm is shown in Figure 7b, from which the decay rate constant (k_{decay}) was estimated to be 3.2×10^{11} s^{-1}, which corresponds to a lifetime (τ_{decay}) of 3 ps. Similar subpicosecond transient absorption spectra were observed for C_{60}−*ortho*-TTF in toluene ($k_{decay} = 1.3 \times 10^{11}$ s^{-1}; $\tau_{decay} = 8$ ps) and C_{60}−*meta*-TTF in benzonitrile and toluene ($k_{decay} = 1.0 \times 10^{11}$ s^{-1}; $\tau_{decay} = 10$ ps). As was observed in the broad absorption band in the 800−1200 nm region, the S_1-S_n transition of C_{60} (980 nm)[45] and the radical anion of the C_{60} moieties (1000 nm)[43] were reported. It is reasonable to consider that [($C_{60}^{\delta-}$−*ortho*-$TTF^{\delta+}$)*] and [($C_{60}^{\delta-}$−*meta*-$TTF^{\delta+}$)*] showed broad absorption in this region, because the absorption band of the $C_{60}^{\bullet-}$ moiety centered at 1000 nm broadens by the interaction with the nearby $TTF^{\delta+}$ moiety. Because both the process of the internal relaxation from ($^1C_{60}^*$−*ortho*-TTF)/($^1C_{60}^*$−*meta*-TTF) to [($C_{60}^{\delta-}$−*ortho*-$TTF^{\delta+}$)*]/[($C_{60}^{\delta-}$−*meta*-$TTF^{\delta+}$)*] and the CR process from [($C_{60}^{\delta-}$-*ortho*-$TTF^{\delta+}$)*]/[($C_{60}^{\delta-}$-*meta*-$TTF^{\delta+}$)*] to ($C_{60}^{\delta-}$−*ortho*-$TTF^{\delta+}$)/($C_{60}^{\delta-}$−*meta*-$TTF^{\delta+}$) are very fast processes, it is difficult to discriminate between these processes. Both decay processes may be included in the decay of the broad absorption in the 800−1200 nm region. The internal relaxation process from ($^1C_{60}^*$−*ortho*-TTF)/($^1C_{60}^*$−*meta*-TTF) to [($C_{60}^{\delta-}$−*ortho*-$TTF^{\delta+}$)*]/[($C_{60}^{\delta-}$−*meta*-$TTF^{\delta+}$)*] occurs usually within ca. 1 ps;[46] therefore, the rapid decay process (k_{decay}) can be attributed mainly to the CR process from [($C_{60}^{\delta-}$−*ortho*-$TTF^{\delta+}$)*]/[($C_{60}^{\delta-}$−*meta*-$TTF^{\delta+}$)*] to ($C_{60}^{\delta-}$−*ortho*-$TTF^{\delta+}$)/($C_{60}^{\delta-}$−*meta*-$TTF^{\delta+}$).

C_{60}−*para*-TTF showed a slightly sharper absorption peak at ~980 nm, with an 850-nm band just after the photoexcitation in benzonitrile, as shown in Figure 8a. The time profiles at 980 nm (Figure 8b) indicate that the k_{decay} values were estimated to be $8.2 \times 10^{10}-8.5 \times 10^{10}$ s^{-1} ($\tau_{decay} = 12$ ps) in benzonitrile and in toluene for C_{60}−*para*-TTF. The broad absorption bands in the region of 800−1100 nm with a peak at 980 nm of C_{60}−*para*-TTF can be thought as the overlap of ($^1C_{60}^*$−*para*-TTF) and $C_{60}^{\bullet-}$−*para*-$TTF^{\bullet+}$; the sharper peak at 980 nm may be due to the weaker interaction between the $C_{60}^{\bullet-}$ and $TTF^{\bullet+}$ moieties in $C_{60}^{\bullet-}$−*para*-$TTF^{\bullet+}$. Slightly small k_{decay} values for $C_{60}^{\bullet-}$−*para*-$TTF^{\bullet+}$ suggest that CR occurs through the bond, whereas large k_{decay} values for ($C_{60}^{\delta-}$−*ortho*-$TTF^{\delta+}$)* and ($C_{60}^{\delta-}$−*meta*-$TTF^{\delta+}$)* suggest spatial back electron transfer from $C_{60}^{\delta-}$ to the proximal $TTF^{\delta+}$.[7,28,47,48]

2.8. Energy Diagrams of C_{60}−*X*-TTF. Photoinduced processes of C_{60}−*X*-TTF (*X* = *ortho* and *meta*) and C_{60}−*para*-TTF are schematically summarized in the energy diagrams shown in Figure 9a and b, respectively, in which the former has appreciable CT interaction, whereas the latter has very weak CT interaction. The energy levels of ($C_{60}^{\delta-}$−*ortho*-$TTF^{\delta+}$)* and ($C_{60}^{\delta-}$−*meta*-$TTF^{\delta+}$)* can be estimated from the CT bands in the steady-state absorption spectra to be 1.65−1.68 eV, which are lower than that of the $^1C_{60}^*$ moiety by ca. 0.1 eV. These ($C_{60}^{\delta-}$−*ortho*-$TTF^{\delta+}$)* and ($C_{60}^{\delta-}$−*meta*-$TTF^{\delta+}$)* species are generated from $^1C_{60}^*$−*ortho*-TTF and $^1C_{60}^*$−*meta*-TTF within ca. 1 ps after photoexcitation,[46] which is the predominant path, suppressing the Φ_T values of $^3C_{60}^*$−*ortho*-TTF and $^3C_{60}^*$−*meta*-TTF.

On the other hand, the free-energy change for the CS ($C_{60}^{\bullet-}$−*para*-$TTF^{\bullet+}$) can be calculated to be ca. 0.83 eV in benzonitrile and 0.20 eV in toluene, as listed in Table 2. In benzonitrile, the free-energy change for the CS process (0.83 eV) via $^1C_{60}^*$−*para*-TTF may be almost a top region of the Marcus parabola for fullerene-donor dyads, because similar values (0.75−0.85 eV) were reported for the reorganization energy;[49] thus, the CS process may be extremely fast. The rapid CS process suppresses the formation of $^3C_{60}^*$−*para*-TTF. In toluene, the CS state

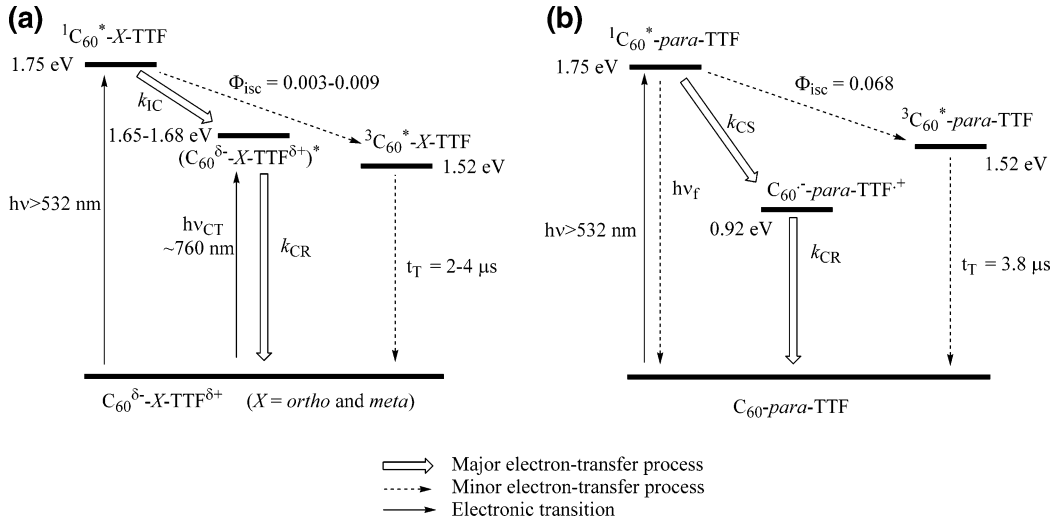

Figure 9. Energy diagram for electron-transfer processes and triplet formation processes of (a) C_{60}−*X*-TTF (*X* = *ortho* and *meta*) and (b) C_{60}−*para*-TTF; the energy level of the CS state in benzonitrile is depicted.

($C_{60}^{\bullet-}$−*para*-$TTF^{\bullet+}$) is at almost the same level as the $^3C_{60}^*$−*para*-TTF, which suggests slower CS via $^1C_{60}^*$−*para*-TTF in the normal region and slower CR in the inverted region in the Marcus parabola, compared to the case in benzonitrile; however, the short distance between the C_{60} and TTF moieties may make the relaxation via the CS state a major process and give fast rates for both the CS and CR processes.

2.9. Comparison with Other C_{60}−TTF Dyads. Compared with the C_{60}−TTF dyads reported previously, whose lifetimes of CS states are usually in the nanosecond range for C_{60}−TTF and several hundreds of nanoseconds for C_{60}−exTTF, the lifetime of CS states of C_{60}−*para*-TTF in benzonitrile is rather short, probably because of short linkage, in addition to the stronger intramolecular interaction than those in the previous C_{60}−TTF dyads. However, González et al. reported that methanofullerene-based C_{60}−exTTF dyads and triads showed CS states lifetimes on the order of picoseconds (210−280 ps in toluene and 55−90 ps in benzonitrile);[31] compared to these lifetimes, the lifetime of C_{60}−*para*-TTF is still short. The modification of C_{60}−*X*-TTF to provide long-lived CS states that retain their intramolecular CT interaction between the C_{60} and TTF moieties is a continuing issue in our laboratory.

3. Conclusion

We have described the synthesis of novel methanofullerene-based dyads of C_{60} and TTF (C_{60}−*X*-TTF, *X* = *ortho*, *meta*, and *para*). Unlike the previous C_{60}−TTF dyads, the present dyads showed pronounced intramolecular charge transfer (CT) absorption bands in the steady-state absorption spectra, suggesting the partial CT character, which is depicted as $C_{60}^{\delta-}$−*X*-$TTF^{\delta+}$ in the ground state. The magnitude of the CT absorption bands follows the order C_{60}−*ortho*-TTF > C_{60}−*meta*-TTF ≫ C_{60}−*para*-TTF, which corresponds to the strength of the intramolecular interaction between the C_{60} and TTF moieties, plausibly explained by the proximity between the two chromophores. The optimized molecular structures obtained by the ab initio calculations support the same order of proximity. The extremely low fluorescence intensity and T−T absorption intensity of C_{60}−*X*-TTF suggest the presence of efficient CT and CS paths from $^1C_{60}^*$−*X*-TTF. In the case of appreciable CT interaction observed for C_{60}−*ortho*-TTF and C_{60}−*meta*-TTF, the excited CT state—depicted as $(C_{60}^{\delta-}$−*X*-$TTF^{\delta+})^*$—may be produced via $^1C_{60}^*$−*X*-TTF; $(C_{60}^{\delta-}$−*X*-$TTF^{\delta+})^*$ may return to the ground CT state ($C_{60}^{\delta-}$−*X*-$TTF^{\delta+}$) with fast back electron transfer through spatially. On the other hand, C_{60}−*para*-TTF undergoes charge separation to form the CS state ($C_{60}^{\bullet-}$−*para*-$TTF^{\bullet+}$), which returns to C_{60}−*para*-TTF with slightly slower back electron transfer than those for C_{60}−*ortho*-TTF and C_{60}−*meta*-TTF, probably via a through-bond mechanism.

4. Experimental Section

4.1. General and Materials. ^{1}H NMR and ^{13}C NMR spectra were measured on a JEOL model JNM-LA400 spectrometer. Matrix-assisted laser desorption ionization−time of flight (MALDI−TOF) mass spectroscopy (MS) spectra were recorded with a Shimazu Kompact PROBE, using α-cyano-4-hydroxycinnamic acid (CHCA) as the matrix. Steady-state absorption and fluorescence spectra were measured on a Hitachi model U-3500 spectrophotometer and a Shimadzu model RF-5300 PC spectrofluorophotometer that was equipped with a photomultiplier tube with high sensitivity up to 860 nm, respectively.

All reactions were performed in a dry reaction vessel under nitrogen. Column chromatography was performed on silica gel (60 spherical 100−210 μm). All solvents and chemicals were reagent-grade, purchased commercially, and used without further purification unless otherwise noted. Tetrahydrofuran (THF) was distilled from sodium benzophenone ketyl under a nitrogen atmosphere prior to use, and toluene was distilled from CaH_2. Tetrabutylammonium perchlorate, which was used for electrochemical measurements, was recrystallized from ethanol (EtOH) before use.

4.2. General Procedure for Synthesis of Acetals (3a−c). The synthesis of **3a** is representative. A methanol solution of NaOMe (28% × 594 mg, 3.08 mmol) was added dropwise to a suspension of 4′-cyanoethyl-5′-methyl-4,5-ethylenedithiotetrathiafulvalene (**1**) (362 mg, 1.01 mmol) in MeOH (30 mL), under a nitrogen atmosphere at room temperature. After stirring for 3 h, a methanol solution of acetal **2a** was added dropwise. The reaction mixture was stirred for an additional 2 h and then water was added. The mixture was extracted with several portions of CH_2Cl_2 and washed with water. The extracts were dried over $MgSO_4$ and concentrated under reduced pressure. Purification by column chromatography on silica gel, using a CH_2Cl_2−*n*-hexane (4:1) mixture as an eluent, was performed, to afford 525 mg (0.96 mmol) of **3a** (96% yield).

*4.2.1. 5′-{3-[2-(1,3-Dioxan-2-yl)phenyl]propylthio}-4′-methyl-4,5-ethylenedithiotetrathiafulvalene (**3a**).* Red oil. ^{1}H NMR ($CDCl_3$): δ 1.40 (d, *J* = 13.6 Hz, 1H), 1.91 (m, 2H), 2.11 (s,

3H), 2.17−2.26 (m, 1H), 2.73−2.82 (m, 4H), 3.25 (s, 4H), 3.96 (t, J = 10.4 Hz, 2H), 4.23 (dd, J = 4.8, 11.2 Hz, 2H), 5.61 (s, 1H), 7.14 (d, J = 6.4 Hz, 1H), 7.20−7.27 (m, 2H), 7.58 (d, J = 6.8 Hz, 1H). ^{13}C NMR ($CDCl_3$): δ 15.38, 25.85, 30.28, 31.28, 31.48, 35.85, 67.58, 100.07, 105.59, 114.04, 115.57, 119.47, 126.50, 126.68, 128.89, 129.58, 134.50, 136.46, 138.76. MS(EI): m/z 534(M^+). Anal. Calcd for $C_{22}H_{24}O_2S_7$: C, 48.49; H, 4.44. Found: C, 48.17; H, 4.56.

*4.2.2. 5′-{3-[3-(1,3-Dioxan-2-yl)phenyl]propylthio}-4′-methyl-4,5-ethylenedithiotetrathiafulvalene (**3b**).* Red oil. ^{1}H NMR ($CDCl_3$): δ 1.43 (d, J = 13.6 Hz, 1H), 1.90 (m, 2H), 2.13 (s, 3H), 2.16−2.24 (m, 1H), 2.69 (m, 4H), 3.24 (s, 4H), 3.98 (t, 2H), 4.25 (dd, J = 4.0, 11.2 Hz, 2H), 5.48 (s, 1H), 7.13 (d, J = 7.6 Hz, 1H), 7.25−7.31 (m, 3H). ^{13}C NMR ($CDCl_3$): δ 15.35, 25.78, 30.24, 30.98, 34.29, 35.39, 67.40, 101.60, 105.32, 114.03, 115.46, 119.34, 123.85, 125.96, 128.39, 128.94, 134.78, 138.89, 141.03. MS(EI): m/z 543(M^+). Anal. Calcd for $C_{22}H_{24}O_2S_7$: C, 48.49; H, 4.44. Found: C, 47.45; H, 4.32.

*4.2.3. 5′-{3-[4-(1,3-Dioxan-2-yl)phenyl]propylthio}-4′-methyl-4,5-ethylenedithiotetrathiafulvalene (**3c**).* Red oil. ^{1}H NMR ($CDCl_3$): δ 1.43 (d, J = 13.7 Hz, 1H), 1.92−1.96 (m, 2H), 2.13 (s, 3H), 2.19−2.24 (m, 1H), 2.70 (t, J = 6.0 Hz, 2H), 2.80 (t, J = 7.4 Hz, 2H), 3.26 (s, 4H), 3.97 (t, J = 12.3 Hz, 2H), 4.24 (dd, J = 4.8, 10.4 Hz, 2H), 5.28 (s, 1H), 7.33 (d, J = 8.0 Hz, 2H), 7.80 (d, J = 8.0 Hz, 2H). ^{13}C NMR ($CDCl_3$): δ 15.35, 25.77, 30.21, 31.02, 34.06, 35.18, 67.35, 101.59, 113.91, 119.28, 126.12, 128.20, 129.12, 130.02, 135.01, 136.64, 141.62. MS(EI): m/z 543(M^+). Anal. Calcd for $C_{22}H_{24}O_2S_7$: C, 48.49; H, 4.44. Found: C, 48.14; H, 4.41.

4.3. General Procedure for Synthesis of Aldehydes (4a−c). The synthesis of **4a** is representative. A mixture of **3a** (360 mg, 0.66 mmol) and pyridinium *p*-toluenesulfonic acid (5 mg, 0.02 mmol) in acetone (25 mL) and water (5 mL) was refluxed under nitrogen overnight, and acetone was removed under reduced pressure. The residue was extracted with CH_2Cl_2 and washed with water. Purification by column chromatography on silica gel, using a CH_2Cl_2−*n*-hexane (2:1) mixture as an eluent, was performed to afford 250 mg (0.59 mmol) of **4a** (89% yield).

*4.3.1. 5′-[3-(2-Formylphenyl)propylthio]-4′-methyl-4,5-ethylenedithiotetrathiafulvalene (**4a**).* Red oil. ^{1}H NMR ($CDCl_3$): δ 1.88−1.95 (m, 1H), 2.14 (s, 3H), 2.75 (t, J = 7.0 Hz, 2H), 3.14 (t, J = 7.4 Hz, 2H), 3.28 (s, 4H), 7.28 (d, J = 7.2 Hz, 1H), 7.40 (t, J = 7.6 Hz, 1H), 7.52 (t, J = 7.2 Hz, 1H), 7.81 (d, J = 6.8 Hz, 1H), 10.21 (s, 1H). ^{13}C NMR ($CDCl_3$): δ 15.34, 30.23, 31.33, 35.49, 105.59, 114.05, 119.19, 126.83, 131.12, 133.11, 133.77, 134.78, 143.65, 192.48. MS(EI): m/z 485(M^+). Anal. Calcd for $C_{19}H_{18}OS_7$: C, 46.88; H, 3.73. Found: C, 46.72; H, 3.72.

*4.3.2. 5′-[3-(3-Formylphenyl)propylthio]-4′-methyl-4,5-ethylenedithiotetrathiafulvalene (**4b**).* Red oil. ^{1}H NMR ($CDCl_3$): δ 1.91−1.97 (m, 2H), 2.14 (s, 3H), 2.41 (t, J = 7.0 Hz, 2H), 2.71 (t, J = 7.6 Hz, 2H), 3.29 (s, 4H), 7.45−7.47 (m, 2H), 7.69−7.74 (m, 2H), 10.00 (s, 1H). ^{13}C NMR ($CDCl_3$): δ 15.40, 30.28, 30.90, 34.04, 35.20, 105.85, 114.04, 115.18, 119.11, 127.93, 129.36, 134.86, 135.02, 136.73, 142.15, 192.38. MS(EI): m/z 485(M^+). Anal. Calcd for $C_{19}H_{18}OS_7$: C, 46.88; H, 3.73. Found: C, 46.67; H, 3.77.

*4.3.3. 5′-[3-(4-Formylphenyl)propylthio]-4′-methyl-4,5-ethylenedithiotetrathiafulvalene (**4c**).* Red oil. ^{1}H NMR ($CDCl_3$): δ 1.88−1.98 (m, 2H), 2.13 (s, 3H), 2.70 (t, J = 7.4 Hz, 2H), 2.80 (t, J = 7.4 Hz, 2H), 3.28 (s, 4H), 7.33 (d, J = 7.6 Hz, 2H), 7.80 (d, J = 8.2 Hz, 2H), 9.97(s, 1H). ^{13}C NMR ($CDCl_3$): δ 15.35, 30.23, 30.65, 34.50, 35.18, 105.93, 113.93, 114.03, 115.02, 119.02, 129.13, 130.04, 134.76, 135.01, 148.37, 191.82. MS(EI): m/z 485(M^+). Anal. Calcd for $C_{19}H_{18}OS_7$: C, 46.88; H, 3.73. Found: C, 46.85; H, 3.84.

4.4. General Procedure for Synthesis of Hydrazone (5a−c). The synthesis of **5a** is representative. A mixture of **4a** (250 mg, 0.59 mmol) and *p*-toluenesulfonyl hydrazide (172 mg, 0.92 mmol) in THF (30 mL) was refluxed under nitrogen for 2 h. After concentration under reduced pressure, the residue was subjected to column chromatography on silica gel, using CH_2Cl_2 as an eluent, to afford 303 mg (0.47 mmol) of **5a** (80% yield).

*4.4.1. 2-[3-(4′-Methyl-4,5-ethylenedithiotetrathiafulvalen-5′-ylthio)propyl]benzaldehyde p-toluenesulfonylhydrazone (**5a**).* Orange solid; mp, 97−98 °C. ^{1}H NMR ($CDCl_3$): δ 1.78 (t, J = 7.2 Hz, 1H), 2.10 (s, 3H), 2.40 (s, 3H), 2.64 (t, J = 7.0 Hz, 2H), 2.80 (t, J = 7.6 Hz, 2H), 3.27 (s, 4H), 7.12 (d, J = 8.0 Hz, 1H), 7.19 (t, J = 7.4 Hz, 1H), 7.27 (d, J = 7.2 Hz, 1H), 7.31 (d, J = 7.6 Hz, 2H), 7.63 (d, J = 7.6 Hz, 1H), 7.87 (d, J = 8.4 Hz, 2H), 8.02 (s, 1H), 8.57 (s, 1H). ^{13}C NMR ($CDCl_3$): δ 15.40, 21.67, 30.29, 30.98, 31.64, 35.39, 114.09, 119.23, 126.65, 128.05, 128.41, 129.81, 130.30, 130.86, 134.84, 135.43, 140.29, 144.39, 146.71. Anal. Calcd for $C_{26}H_{26}N_2O_2S_8$: C, 47.67; H, 4.00; N, 4.28. Found: C, 47.17; H, 4.43; N, 3.91.

*4.4.2. 3-[3-(4′-Methyl-4,5-ethylenedithiotetrathiafulvalen-5′-ylthio)propyl]benzaldehyde p-toluenesulfonylhydrazone (**5b**).* Orange solid; mp, 77−78 °C. ^{1}H NMR ($CDCl_3$): δ 1.84−1.89 (m, 2H), 2.11 (s, 3H), 2.38 (s, 3H), 2.63−2.69 (m, 4H), 3.27 (s, 4H), 7.15 (d, J = 7.6 Hz, 1H), 7.24 (t, J = 7.6 Hz, 1H), 7.29 (d, J = 7.6 Hz, 2H), 7.35 (s, 1H), 7.40 (d, J = 7.6 Hz, 1H), 7.73 (s, 1H), 7.87 (d, J = 8.4 Hz, 2H), 8.53 (s, 1H). ^{13}C NMR ($CDCl_3$): δ 15.38, 21.62, 30.24, 30.92, 33.98, 35.10, 105.44, 114.01, 115.26, 125.15, 127.49, 127.95, 128.80, 129.66, 130.68, 133.36, 134.94, 135.37, 141.54, 144.24, 147.98. Anal. Calcd for $C_{26}H_{26}N_2O_2S_8$: C, 47.67; H, 4.00; N, 4.28. Found: C, 46.35; H, 4.00; N, 4.13.

*4.4.3. 4-[3-(4′-Methyl-4,5-ethylenedithiotetrathiafulvalen-5′-ylthio)propyl]benzaldehyde p-toluenesulfonylhydrazone (**5c**).* Red solid; mp, 165−166 °C. ^{1}H NMR ($CDCl_3$): δ 1.84−1.88 (m, 2H), 2.13 (s, 3H), 2.41 (s, 3H), 2.65−2.73 (m, 4H), 3.30 (s, 4H), 7.08 (d, J = 8.1 Hz, 2H), 7.24 (d, J = 8.6 Hz, 2H), 7.39 (d, J = 8.1 Hz, 2H), 7.63 (s, 1H), 7.76 (d, J = 8.3 Hz, 2H), 8.16 (s, 1H). ^{13}C NMR ($CDCl_3$): δ 15.37, 21.64, 30.31, 30.85, 34.22, 35.21, 100.82, 127.64, 127.98, 128.87, 129.73, 131.16, 134.91, 135.42, 141.33, 143.91, 144.27, 146.46, 147.94. Anal. Calcd for $C_{26}H_{26}N_2O_2S_8$: C, 47.67; H, 4.00; N, 4.28. Found: C, 47.20; H, 4.02; N, 4.24.

4.5. General Procedure for Synthesis of C_{60}−*X*-TTF. The synthesis of C_{60}−*ortho*-TTF is representative. A methanol solution of NaOMe (28% × 102 mg, 0.53 mmol) was added to a solution of **5a** (303 mg, 0.47 mmol) in methanol (30 mL), and the mixture was refluxed for 10 min under nitrogen. A toluene (distilled from CaH_2, 20 mL) solution of C_{60} (162 mg, 0.23 mmol) was successively added to the refluxing mixture, and the resulting mixture was refluxed for 8 h. After water was added, the mixture was extracted with toluene and washed with water. The extracts were dried over $MgSO_4$, concentrated under reduced pressure, and purified by column chromatography on silica gel, using carbon disulfide as an eluent, to afford 4.8 mg (0.04 mmol) of C_{60}−*ortho*-TTF in 8.4% yield (27% from reacted C_{60}).

4.5.1. 3′-{2-[3-(4′-Methyl-4,5-ethylenedithiotetrathiafulvalen-5′-ylthio)propyl]phenyl}-3′H-cyclopropa[1,9](C$_{60}$−I$_h$)[5,6]-fullerene (C$_{60}$−ortho-TTF). Dark brown solid; mp, 220−222 °C dec. ^{1}H NMR ($CDCl_3$:CS_2 = 1:4): δ 1.91 (m, 2H), 2.08 (s, 3H), 2.65 (t, J = 7.8 Hz, 2H), 2.82 (t, J = 7.6 Hz, 2H), 3.26 (s, 4H), 4.01 (s, 1H), 7.32−7.34 (m, 1H), 7.38−7.40 (m, 2H),

8.26−8.28 (m, 1H). ^{13}C NMR ($CDCl_3$:CS_2 = 1:4): δ 15.20, 29.83, 30.19, 31.17, 32.92, 35.80, 52.42, 105.70, 113.54, 113.63, 114.38, 119.35, 125.13, 126.44, 128.02, 182.77, 129.52, 130.67, 133.92, 134.69, 135.05, 135.86, 136.79, 137.83, 138.19, 138.26, 138.36, 140.02, 140.61, 141.45, 141.52, 141.81, 142.18, 142.42, 142.62, 142.72, 142.88, 143.13, 143.20, 143.34, 143.46, 143.49, 143.61, 144.08, 144.64, 144.68, 147.47. MALDI−TOF-MS (*m*/*z*) 1191(M^+).

4.5.2. 3′-{3-[3-(4′-Methyl-4,5-ethylenedithiotetrathiafulvalen-5′-ylthio)propyl]phenyl}-3′H-cyclopropa[1,9](C60−Ih)[5,6]-fullerene (C60−meta-TTF). Dark brown solid; mp, >308 °C. ^{1}H NMR ($CDCl_3$:CS_2 = 1:4): δ 1.94−2.00 (m, 2H), 2.10 (s, 3H), 2.69 (t, J = 7.2 Hz, 2H), 2.83 (t, J = 7.4 Hz, 1H), 3.26 (s, 4H), 7.21 (d, J = 8.0 Hz, 1H), 7.43 (t, J = 7.6 Hz, 1H), 7.73−7.77(m, 2H). ^{13}C NMR ($CDCl_3$:CS_2 = 1:4): δ 15.19, 29.88, 30.34, 31.13, 31.77, 34.55, 35.18, 53.57, 129.46, 133.92, 135.11, 138.02, 138.13, 138.36, 138.41, 139.61, 139.99, 141.39, 141.52, 141.79, 142.35, 142.39, 142.46, 142.69, 142.81, 142.92, 143.17, 143.28, 143.43, 143.60, 143.63, 143.96, 144.62, 144.67, 147.59. MALDI−TOF-MS (*m*/*z*) 1191(M^+).

4.5.3. 3′-{4-[3-(4′-Methyl-4,5-ethylenedithiotetrathiafulvalen-5′-ylthio)propyl]phenyl}-3′H-cyclopropa[1,9](C60-Ih)[5,6]-fullerene (C60−para-TTF). Dark brown solid; mp, >308 °C. ^{1}H NMR ($CDCl_3$:CS_2 = 1:4): δ 1.97−2.02 (m, 2H), 2.32 (s, 3H), 2.73 (t, J = 7.0 Hz, 2H), 2.81 (t, J = 7.6 Hz, 1H), 3.25 (s, 4H), 7.35 (d, J = 8.4 Hz, 2H), 7.86 (d, J = 8.0 Hz, 2H). ^{13}C NMR ($CDCl_3$:CS_2 = 1:4): δ 15.91, 29.04, 30.06, 30.36, 31.20, 31.81, 34.29, 35.43, 53.43, 106.43, 117.17, 119.42, 123.42, 126.98, 128.01, 128.43, 128.92, 129.22, 130.15, 131.93, 134.35, 135.09, 137.97, 140.70, 141.46, 141.70, 142.38, 142.61, 142.74, 142.87, 142.91, 143.10, 143.23, 143.58, 143.84, 144.62, 147.53. MALDI−TOF-MS (*m*/*z*) 1191(M^+).

4.6. Electrochemical Measurements. Cyclic voltammetry was performed through the application of an electrochemical analyzer (ALS model 600A) at 25 °C in benzonitrile (0.1−0.2 mM) that contained *n*-Bu_4NClO_4 (0.1 M) as a supporting electrolyte at a scan rate of 50 mV s^{-1}, using platinum working and counter electrodes and a saturated calomel electrode (SCE) as the reference electrode. The solution was deaerated with N_2 bubbling before measurements.

4.7. Transient Absorption Measurements. Nanosecond transient absorption measurements were performed using second harmonic generation (SHG) (532 nm) of a Nd:YAG laser (Spectra-Physics, Quanta-Ray GCR-130, 6 ns fwhm) as an excitation source. For transient absorption spectra in the near-IR region (600−1200 nm) and the time profiles, monitoring light from a pulsed xenon lamp was detected with a Ge-APD (Hamamatsu Photonics, B2834).[44] The subpicosecond transient absorption spectra were recorded by the pump and probe method. The sample was excited with 388-nm laser light from the SHG of output from a femtosecond Ti:sapphire regenerative amplifier seeded by the SHG of a europium-dropped fiber (Clark-MXR CPA-2001 plus, 1 kHz, fwhm 150 fs). The monitor white light was generated by focusing the fundamental of laser light on the flowing D_2O/H_2O cell. The transmitted monitor light was detected with a dual metal oxide semiconductor (MOS) linear image sensor (Hamamatsu Photonics, model C6140) or an InGaAs photodiode array (Hamamatsu Photonics, model C5890-128).[50] All the samples in a quartz cell (1 cm × 1 cm) were deaerated by bubbling argon through the solution for 10 min. For subpicosecond measurements, a rotating cell (optical path: 2 mm) was used to avoid any sample degradation and nonlinear effect.

Acknowledgment. This work was partly supported by JSPS, Grants-in-Aid for Scientific Research (Nos. 15550127, 10207202, 11740380, and 12875163), and Industrial Technology Research Grant Program in '02 from New Energy and Industrial Technology Development Organization (NEDO). The authors are also grateful for financial support by the Mitsubishi Foundation, Ishikawa Carbon Foundation, and Core Research for Evolution Science and Technology (CREST) of Japan Science and Technology Agency.

References and Notes

(1) (a) Hirsch, A. *The Chemistry of the Fullerenes*; Thieme: Stuttgart, 1994. (b) Smith, A. B., Ed. *Tetrahedron Symposia-in-Print, Number 60*; Fullerene Chemistry; 1996; p 52. (c) Hirsch, A., Ed. *Top. Curr. Chem.* **1999**, *199*.

(2) (a) Kadish, K. M., Ruoff, R. S., Eds. *Fullerenes: Chemistry, Physics, and Technology*; Wiley Interscience: New York, 2000. (b) Cravino, A.; Sariciftci, N. S. *J. Mater. Chem.* **2002**, *12*, 1931−1943.

(3) (a) Liddell, P. A.; Sumida, J. P.; Macpherson, A. N.; Noss, L.; Seely, G. R.; Clark, K. N.; Moore, A. L.; Moore, T. A.; Gust, D. *Photochem. Photobiol.* **1994**, *60*, 537−541. (b) Imahori, H.; Sakata, Y. *Eur. J. Org. Chem.* **1999**, 2445−2457. (c) Gust, D.; Moore, T. A.; Moore, L. *Acc. Chem. Res.* **2001**, *34*, 40−48.

(4) (a) Yu, G.; Gao, J.; Hummelen, J. C.; Wudl, F.; Heeger, A. J. *Science* **1995**, *270*, 1789−1791. (b) Janssen, R. A. J.; Hummelen, J. C.; Lee, K.; Pakbaz, K.; Sariciftci, N. S.; Heeger, A. J.; Wudl, F. *J. Phys. Chem.* **1995**, *103*, 788−793. (c) Kraabel, B.; Hummelen, J. C.; Vacar, D.; Moses, D.; Sariciftci, N. S.; Heeger, A. J.; Wudl, F. *J. Phys. Chem.* **1996**, *100*, 4267−4273. (d) Prato, M. *J. Mater. Chem.* **1997**, *17*, 1097−1109. (e) Diederich, F.; Gómez-López, M. *Chem. Soc. Rev.* **1999**, *28*, 263−277. (f) Nierengarten, J.-F.; Eckert, J.-F.; Felder, D.; Nicoud, J.-F.; Armaroli, N.; Marconi, G.; Vicinelli, V.; Boudon, C.; Gisselbrecht, J.-P.; Gross, M.; Hadziioannou, G.; Krasnikov, V.; Ouali, L.; Echegoyen, L.; Liu, S.-G. *Carbon* **2000**, *38*, 1587−1598. (g) Brabec, C. J.; Cravino, A.; Zerza, G.; Sariciftci, N. S.; Kiebooms, R.; Vanderzande, D.; Hummelen, J. C. *J. Phys. Chem. B* **2001**, *105*, 1528−1536. (h) Brabec, C. J.; Sariciftci, N. S.; Hummelen, J. C. *Adv. Funct. Mater.* **2001**, *11*, 15−26.

(5) (a) Prato, M.; Maggini, M.; Giacometti, C.; Scorrano, G.; Sandonà, G.; Farnia, G. *Tetrahedron* **1996**, *52*, 5221−5234. (b) Echegoyen, L.; Echegoyen, L. E. *Acc. Chem. Res.* **1998**, *31*, 593−601.

(6) (a) Williams, R. M.; Zwier, J. M.; Verhoeven, W. *J. Am. Chem. Soc.* **1995**, *117*, 4093−4099. (b) Lawson, J. M.; Oliver, A. M.; Rothenfluh, D. F.; An, Y.-Z.; Ellis, G. A.; Ranasinghe, M. G.; Khan, S. I.; Franz, A. G.; Ganapathi, P. S.; Shephard, M. J.; Paddon-Row, M. N.; Rubin, Y. *J. Am. Chem. Soc.* **1996**, *61*, 5032−5054. (c) Williams, R. M.; Koeberg, M.; Lawson, J. M.; An, Y.-Z.; Rubin, Y.; Paddon-Row, M. N.; Verhoeven, J. W. *J. Am. Chem. Soc.* **1996**, *61*, 5055−5062. (d) Imahori, H.; Sakata, Y. *Adv. Mater.* **1997**, *9*, 537−546. (e) Martín, N.; Sánchez, L.; Illescas, B.; Pérez, I. *Chem. Rev.* **1998**, *98*, 2527−2547.

(7) (a) Guldi, D. M.; Prato, M. *Acc. Chem. Res.* **2000**, *33*, 695−703. (b) Guldi, D. M. *Chem. Commun.* **2000**, 321−327.

(8) (a) Nierengarten, J.-F.; Eckert, J.-F.; Nicoud, J.-F.; Ouali, L.; Krasnikov, V.; Hadziioannou, G. *Chem. Commun.* **1999**, 617−618. (b) Kamat, P. V.; Barazzouk, S.; Hotchandani, S.; Thomas, K. G. *Chem. Eur. J.* **2000**, *6*, 3914−3921. (c) Eckert, J.-F.; Nicoud, J.-F.; Nierengarten, J.-F.; Liu, S.-G.; Echegoyen, L.; Barigelletti, F.; Armaroli, N.; Ouali, L.; Krasnikov, V.; Hadziioannou, G. *J. Am. Chem. Soc.* **2000**, *122*, 7467−7479.

(9) (a) Imahori, H.; Azuma, T.; Ajavakom, A.; Norieda, H.; Yamada, H.; Sakata, Y. *J. Phys. Chem. B* **1999**, *103*, 7233−7237. (b) Imahori, H.; Yamada, H.; Nishimura, Y.; Yamazaki, I.; Sakata, Y. *J. Phys. Chem. B* **2000**, *104*, 2099−2108. (c) Luo, C.; Guldi, D. M.; Maggini, M.; Menna, E.; Mondini, S.; Kotov, N. A.; Prato, M. *Angew. Chem., Int. Ed.* **2000**, *39*, 3905−3909. (d) Imahori, H.; Norieda, H.; Yamada, H.; Nishimura, Y.; Yamazaki, I.; Sakata, Y.; Fukuzumi, S. *J. Am. Chem. Soc.* **2001**, *123*, 100−110. (e) Hirayama, D.; Takimiya, K.; Aso, Y.; Otsubo, T.; Hasobe, T.; Yamada, H.; Imahori, H.; Fukuzumi, S.; Sakata, Y. *J. Am. Chem. Soc.* **2002**, *124*, 532−533.

(10) (a) Deuchert, K.; Hünig, S. *Angew. Chem., Int. Ed. Engl.* **1978**, *17*, 875−886. (b) Hünig, S.; Berneth, H. *Top. Curr. Chem.* **1980**, *92*, 1−44.

(11) (a) Ishiguro, T.; Yamaji, K.; Saito, G. *Organic Superconductors*, 2nd ed.; Springer Series in Solid-State Sciences, No. 88; Fulde, P., Ed.; Springer: Berlin, 1998. (b) Williams, J. M.; Ferraro, J. R.; Thorn, R. J.; Carlson, K. D.; Geiser, U.; Wang, H. H.; Kini, A. M.; Wangbo, M.-H. *Organic Superconductors (Including Fullerenes): Synthesis, Structure, Properties and Theory*; Prentice Hall: Englewood Cliffs, NJ, 1992.

(12) (a) Martín, N.; Sánchez, L.; Seoane, C.; Andreu, R.; Garín, J.; Orduna, J. *Tetrahedron Lett.* **1996**, *37*, 5979−5982. (b) Martín, N.; Sánchez, L.; Herranz, M. A.; Guldi, D. M. *J. Phys. Chem. A* **2000**, *104*, 4648−4657.

(13) (a) Martín, N.; Sánchez, L.; Guldi, D. M. *Chem. Commun.* **2000**, 113−114. (b) Martín, N.; Pérez, I.; Sánchez, L.; Seoane, C. *J. Org. Chem.* **1997**, *62*, 5690−5695. (c) Herranz, M. A.; Martín, N.; Sánchez, L.; Seoane, C.; Guldi, D. M. *J. Organomet. Chem.* **2000**, *599*, 2−7.

(14) (a) Guldi, D. M.; González, S.; Martín, N.; Antón, A.; Garín, J.; Orduna, J. *J. Org. Chem.* **2000**, *65*, 1978−1983. (b) González, S.; Martín, N.; Swartz, A.; Guldi, D. M. *Org. Lett.* **2003**, *5*, 557−560.

(15) Herranz, M. A.; Illescas, B.; Martín, N.; Luo, C.; Guldi, D. M. *J. Org. Chem.* **2000**, *65*, 5728−5738.

(16) Prato, M.; Maggini, M.; Giacometti, C.; Scorrano, G.; Sandonà, G.; Farina, G. *Tetrahedron Lett.* **1996**, *52*, 5221−5234.

(17) Simonsen, K. B.; Konovalov, V. V.; Konovalova, T. A.; Kawai, T.; Cava, M. P.; Kispert, L. D.; Metzger, R. M.; Becher, J. *J. Chem. Soc., Perkin Trans. 2* **1999**, 657−665.

(18) (a) Boulle, C.; Rabreau, J.-M.; Hudhomme, P.; Cariou, M.; Jubault, M.; Gorgues, A. *Tetrahedron Lett.* **1997**, *38*, 3909−3910. (b) Hudhomme, P.; Boulle, C.; Rabreau, J.-M.; Cariou, M.; Jubault, M.; Gorgues, A. *Synth. Met.* **1998**, *94*, 73−75. (c) Sahraoui, B.; Kityk, I. V.; Hudhomme, P.; Gorgues, A. *J. Phys. Chem. B* **2001**, *105*, 6295−6299. (d) Olejniczak, I.; Graja, A.; Bogucki, A.; Golub, M.; Hudhomme, P.; Gorgues, A.; Kreher, D.; Cariou, M. *Synth. Met.* **2002**, *126*, 263−268.

(19) (a) Kreher, D.; Liu, S.-G.; Cariou, M.; Hudhomme, P.; Gorgues, A.; Mas, M.; Veciana, J.; Rovira, C. *Tetrahedron Lett.* **2001**, *42*, 3447−3450. (b) Liu, S.-G.; Kreher, D.; Hudhomme, P.; Levillain, E.; Cariou, M.; Delaunay, J.; Gorgues, A.; Vidal-Gancedo, J.; Veciana, J.; Rovira, C. *Tetrahedron Lett.* **2001**, *42*, 3717−3720.

(20) (a) Llacay, J.; Mas, M.; Molins, E.; Veciana, J.; Powell, D.; Rovira, C. *Chem. Commun.* **1997**, 659−660. (b) Llacay, J.; Veciana, J.; Vidal-Gancedo, J.; Bourdelande, J.-L.; González-Moreno, R.; Rovira, C. *J. Org. Chem.* **1998**, *63*, 5201−5210. (c) Mas-Torrent, M.; Rodrígues-Mias, R. A.; Solà, M.; Molins, M. A.; Pons, M.; Vidal-Gancedo, J.; Veciana, J.; Rovira, C. *J. Org. Chem.* **2002**, *67*, 566−575.

(21) Liu, S.-G.; Echegoyen, L. *Eur. J. Org. Chem.* **2000**, 1157−1163.

(22) (a) Allard, E.; Delaunay, J.; Cheng, F.; Cousseau, J.; Ordúna, J.; Garín, J. *Org. Lett.* **2001**, *3*, 3503−3506. (b) Allard, E.; Cousseau, J.; Ordúna, J.; Garín, J.; Luo, H.; Araki, Y.; Ito, O. *Phys. Chem. Chem. Phys.* **2002**, *4*, 5944−5951.

(23) Herranz, M. A.; Martín, N. *Org. Lett.* **1999**, *1*, 2005−2007.

(24) Ravaine, S.; Delhaès, P.; Leriche, P.; Sallé, M. *Synth. Met.* **1997**, *87*, 93−95.

(25) Zeng, P.; Liu, Y.; Zhang, D.; Yang, C.; Li, Y.; Zhu, D. *J. Phys. Chem. Solids* **2000**, *61*, 1111−1117.

(26) Segura, J. L.; Priego, E. M.; Martín, N.; Luo, C.; Guldi, D. M. *Org. Lett.* **2000**, *2*, 4021−4024.

(27) Segura, J. L.; Priego, E. M.; Martín, N. *Tetrahedron Lett.* **2000**, *41*, 7737−7741.

(28) Martín, N.; Sánchez, L.; Illescas, B.; González, S.; Herranz, M. A.; Guldi, D. M. *Carbon* **2000**, *38*, 1577−1585.

(29) Kreher, D.; Cariou, M.; Liu, S.-G.; Levillain, E.; Veciana, J.; Rovira, C.; Gorgues, A.; Hudhomme, P. *J. Mater. Chem.* **2002**, *12*, 2137−2159.

(30) (a) Liddell, P. A.; Kodis, G.; de la Garza, L.; Bahr, J. L.; Moore, A. L.; Moore, T. A.; Gust, D. *Helv. Chim. Acta* **2001**, *84*, 2765−2783. (b) Kodis, G.; Liddell, P. A.; de la Garza, L.; Moore, A. L.; Moore, T. A.; Gust, D. *J. Mater. Chem.* **2002**, *12*, 2100−2108.

(31) (a) González, S.; Martín, N.; Guldi, D. M. *J. Org. Chem.* **2003**, *68*, 779−791. (b) González, S.; Martín, N.; Swartz, A.; Guldi, D. M. *Org. Lett.* **2003**, *5*, 557−560.

(32) Burley, G. A.; Avent, A. G.; Boltalina, O. V.; Gol'dt, I. V.; Guldi, D. M.; Marcaccio, M.; Paolucci, F.; Paolucci, D.; Taylor, R. *Chem. Commun.* **2003**, 148−149.

(33) Sánchez, L.; Pérez, I.; Martín, N.; Guldi, D. M. *Chem. Eur. J.* **2003**, *9*, 2457−2468.

(34) (a) Diederich, F.; Thilgen, C. *Science* **1996**, *271*, 317−323. (b) Diederich, F.; Isaacs, L.; Philip, D. *Chem. Soc. Rev.* **1994**, 243−255.

(35) 4-Cyanoethylthio-5-methyl-4′,5′-ethylenedithiotetrathiafulvalene (**1**) was synthesized in five steps, from the 2-(dimethylamino)-1,3-dithiolium-4-thiolate meso-ion. For details about the meso-ion, see: Jørgensen, M.; Lerstrup, K. A.; Bechgaard, K. *J. Org. Chem.* **1991**, *56*, 5684−5688.

(36) Ma, W.; Slebodnick, C.; Ibers, J. A. *J. Org. Chem.* **1993**, *58*, 6349−6353.

(37) Isaacs, L.; Wehrsig, A.; Diederich, F. *Helv. Chim. Acta* **1993**, *76*, 1231−1250.

(38) (a) Rubin, Y.; Khan, S.; Freedberg, D. I.; Yeretzian, C. *J. Am. Chem. Soc.* **1993**, *115*, 344−345. (b) Lawson, J. M.; Oliver, A. M.; Rothenfluh, D. F.; An, Y.-Z.; Ellis, G. A.; Ranasinghe, M. G.; Khan, S. I.; Franz, A. G.; Ganapathi, P. S.; Shephard, M. J.; Paddon-Row, M. N.; Rubin, Y. *J. Org. Chem.* **1996**, *61*, 5032−5054.

(39) A detector system that used a photomultiplier tube with sensitivity in the near-IR region was used in the present study.

(40) Bell, T. D. M.; Smith, T. A.; Ghiggino, K. P.; Ranasinghe, M. G.; Shephard, M. J.; Paddon-Row, M. *Chem. Phys. Lett.* **1997**, *268*, 223−228.

(41) Frisch, M. J.; Trucks, G. W.; Schlegel, H. B.; Scuseria, G. E.; Robb, M. A.; Cheeseman, J. R.; Zakrzewski, V. G.; Montgomery, J. A., Jr.; Stratmann, R. E.; Burant, J. C.; Dapprich, S.; Millam, J. M.; Daniels, A. D.; Kudin, K. N.; Strain, M. C.; Farkas, O.; Tomasi, J.; Barone, V.; Cossi, M.; Cammi, R.; Mennucci, B.; Pomelli, C.; Adamo, C.; Clifford, S.; Ochterski, J.; Petersson, G. A.; Ayala, P. Y.; Cui, Q.; Morokuma, K.; Rega, N.; Salvador, P.; Dannenberg, J. J.; Malick, D. K.; Rabuck, A. D.; Raghavachari, K.; Foresman, J. B.; Cioslowski, J.; Ortiz, J. V.; Baboul, A. G.; Stefanov, B. B.; Liu, G.; Liashenko, A.; Piskorz, P.; Komaromi, I.; Gomperts, R.; Martin, R. L.; Fox, D. J.; Keith, T.; Al-Laham, M. A.; Peng, C. Y.; Nanayakkara, A.; Challacombe, M.; Gill, P. M. W.; Johnson, B.; Chen, W.; Wong, M. W.; Andres, J. L.; Gonzalez, C.; Head-Gordon, M.; Replogle, E. S.; Pople, J. A. *Gaussian 98*, revision A.11.2; Gaussian, Inc.: Pittsburgh, PA, 2001.

(42) (a) Izuoka, A.; Tachikawa, T.; Sugawara, T.; Suzuki, Y.; Konno, M.; Saito, Y.; Shinohara, H. *J. Chem. Soc., Chem. Commun.* **1992**, 1472−1473. (b) Alam, M. M.; Ito, O.; Sakurai, N.; Moriyama, H. *Fullerene Sci. Technol.* **1998**, *6*, 1007−1024.

(43) Luo, C.; Fujitsuka, M.; Watanabe, A.; Ito, O.; Gan, L.; Huang, Y.; Huang, C. H. *J. Chem. Soc., Faraday Trans.* **1998**, *94*, 527−532.

(44) Komamine, S.; Fujitsuka, M.; Ito, O.; Moriwaki, K.; Miyata, T.; Ohno, T. *J. Phys. Chem. A* **2000**, *104*, 11497−11504.

(45) Watanabe, A.; Ito, O.; Saito, H.; Watanabe, M.; Koishi, M. *J. Chem. Soc., Chem. Commun.* **1996**, 117−118.

(46) (a) Tkachenk, N. V.; Tauber, A. Y.; Grandell, D.; Hynninen, P. H.; Lemmetyinen, H. *J. Phys. Chem. A* **1999**, *103*, 3646−3656. (b) Tkachenk, N. V.; Rantala, L.; Tauber, A. Y.; Helaja, J.; Hynninen, P. H.; Lemmetyinen, H. *J. Am. Chen. Soc.* **1999**, *121*, 9378−9387. (c) Imahori, H.; Tkachenk, N. V.; Vehmanen, V.; Tamaki, K.; Lemmetyinen, H.; Sakata, Y.; Fukuzumu, S. *J. Phys. Chem. A* **2001**, *105*, 1750−1756. (d) Kesti, T. J.; Tkachenk, N. V.; Vehmanen, V.; Yamada, H.; Imahori, H.; Fukuzumu, S. *J. Am. Chem. Soc.* **2002**, *124*, 8067−8077.

(47) (a) Guldi, D. M.; Maggini, M.; Scorrano, G.; Prato, M. *J. Am. Chem. Soc.* **1997**, *119*, 974−980. (b) Guldi, D. M.; Maggini, M.; Scorrano, G.; Prato, M. *Res. Chem. Intermed.* **1997**, *23*, 561−573.

(48) Maggini, M.; Guldi, D. M.; Mondini, S.; Scorrano, G.; Paolucci, F.; Ceroni, P.; Roffia, S. *Chem. Eur. J.* **1998**, *4*, 1992−2000.

(49) Imahori, H.; Tamaki, K.; Guldi, D. M.; Luo, C.; Fujitsuka, M.; Ito, O.; Sakata, Y.; Fukuzumi, S. *J. Am. Chem. Soc.* **2001**, *123*, 2607−2617.

(50) D'Souza, F.; Zandler, M. E.; Smith, P. M.; Deviprasad, G. R.; Arkady, K.; Fujitsuka, M.; Ito, O. *J. Phys. Chem. A* **2002**, *106*, 649−656.